Normal modes and standing waves of scalar field in nonlinear electromagnetic regular anti–de Sitter spacetimes

Kai Lin[*]

School of Geophysics and Geomatics, China University of Geosciences, Wuhan 430074, Hubei, China and Instituto de Física, Universidade de São Paulo, São Paulo, Brazil

Alan B. Pavan[†]

Universidade Federal de Itajubá, Instituto de Física e Química, Itajubá, MG, Brazil

Elcio Abdalla[‡]

Instituto de Física, Universidade de São Paulo, São Paulo, Brazil

(Received 16 March 2024; accepted 8 May 2024; published 7 June 2024)

It has been proven that nonlinear electromagnetic fields can result in regular black holes without singularities in the origin. Consequently, even if the event horizon disappears, this spacetime will not lead to the problem of naked singularities but, instead, becomes a regular spacetime. Thus, it is interesting to study the scalar field evolution in nonlinear electromagnetic regular anti–de Sitter spacetimes in order to analyze its stability. In these regular anti–de Sitter spacetimes, the tortoise coordinate transformation r_* has an upper and lower limit, respectively, and the effective potential of scalar perturbation diverges at maximum r_*, so that the wave cannot penetrate this boundary. On the other hand, at the center of the regular spacetime, the value of the effective potential even with $L = 0$ does not diverge, so the reflection at the center of the wave is equivalent to the reflection on one side of the wave-spreading medium, resulting in a phenomenon of half-wave loss. It means that the process of scalar perturbations in this spacetime is similar to the standing wave vibrations with fixed boundaries in wave mechanics. We will calculate the scalar field normal modes of oscillation and demonstrate the phenomena of standing waves and half-wave loss of nonlinear electromagnetic regular anti–de Sitter spacetimes.

DOI: 10.1103/PhysRevD.109.124019

I. INTRODUCTION

The past decade has undoubtedly been a significant period of development in astronomy in this century. In 2015, LIGO achieved the first direct detection of gravitational waves [1], confirming their existence and validating the presence of merging black holes as sources of gravitational waves. Subsequently, the LIGO-Virgo Collaboration discovered dozens of black hole merger events [2–9]. Additionally, in 2019, the EHT Collaboration announced the first photograph of the central black hole in the M87 galaxy, marking humanity's first image of a black hole. Later, in 2022, the same collaboration presented the imaging of the black hole at the center of our Milky Way. This series of astronomical accomplishments has provided empirical evidence for theoretical physics models that were previously confined to general relativity textbooks, propelling humanity into the era of gravitational wave astronomy and black hole observations.

Moreover, exciting news about new astrophysical phenomena connected with fast radio bursts [10] and their observations [11] opens a new era for the search of types of solutions of general relativity which might explain such phenomena, especially via instabilities [12].

According to general relativity, black holes have singularities. Therein, spacetime curvature becomes infinite and physical theories fail. Fortunately, most black hole solutions in general relativity have an event horizon surrounding the singularity, which is a one-way membrane that prevents the effects of the singularity from reaching regions outside the event horizon. Based on this aspect, Penrose proposed the famous cosmic censorship hypothesis, which suggests that real black hole singularities in the Universe are always enclosed by an event horizon, preventing the singular nature within the event horizon from affecting the outside world [13]. This alleviates the awkward situation for observers. However, the singularity problem has not been fundamentally solved yet, leading to various alternative approaches proposed to address this issue. In 1968, Bardeen first introduced a regular black hole metric [14] that avoids the presence of a singularity, remaining finite at

[*]kailin@if.usp.br
[†]alan@unifei.edu.br
[‡]eabdalla@usp.br

the center and matching the Schwarzschild spacetime at infinity. Later on, it was discovered that Bardeen's regular black hole solution can be constructed using nonlinear electromagnetic theory [15]. Subsequently, a series of regular black hole solutions were proposed [14–21]. More recently, an extensive and complete discussion about proprieties of regular black holes sourced by phantom scalar field and nonlinear electrodynamics was presented in [22] and references therein.

Typically, a four-dimensional static regular black hole can be written in the following form:

$$ds^2 = -f(r)dt^2 + \frac{dr^2}{f(r)} + r^2\left(d\theta^2 + \sin^2\theta d\varphi^2\right) \tag{1.1}$$

and

$$f(r) = 1 - \frac{2\mathcal{M}(r)}{r} = 1 - \frac{2M}{r}C_M(r), \tag{1.2}$$

where M is the Arnowitt-Deser-Misner (ADM) mass of the black hole; thus, we impose that $C_M \to 1$ as $r \to \infty$, and it is requested that $\frac{C_M(r)}{r}$ is finite at $r = 0$ such that the black hole spacetime does not display singularities. In this paper, we choose the natural coordinates $c = G = 1$. So far, within the framework of general relativity, there are several possible ways to construct the regular black holes. The most common approach is to use nonlinear electromagnetic fields. For this purpose, we can consider the potential of a magnetic charge as

$$A_\mu = Q_m \cos(\theta)\delta^\varphi_\mu. \tag{1.3}$$

With this choice, it is possible to express the specific form of the action $\mathcal{L}(F)$ for the nonlinear electromagnetic field and obtain the explicit metric describing the regular black hole spacetime.

On the another hand, we can also obtain a regular black hole by directly constructing the form of the energy-momentum tensor of matter.

It requires satisfying the condition for the energy-momentum tensor [20]: $T^t_t = \rho$, $T^r_r = -p_r$, and $T^\theta_\theta = T^\varphi_\varphi = -p_\perp$, and the equations of state relating pressure p and the energy density ρ are $p_r = -\rho$ and $p_\perp = -\rho - \frac{r}{2}\rho'$. It leads to the following relation:

$$C_M(r) = \frac{4\pi}{M}\int_0^r \rho(x)x^2 dx. \tag{1.4}$$

Then, after setting the form of ρ, we can get the metric of a regular black hole. Many static regular black holes have been proposed through the method. Some works have studied the stability of regular black holes [23–27] analyzing the quasinormal modes, i.e., complex frequencies of oscillation of perturbed spacetime or of probe fields evolving around the black hole. Details about different approaches to calculate quasinormal modes can be obtained in a series of reviews [28–31].

It is worth noting that the advantage of a regular black hole is that the absence of an internal singularity makes the Penrose cosmic censorship hypothesis somewhat redundant in this type of spacetime. Hence, in this spacetime, the magnetic charge can be large enough to make the event horizon disappear, transforming the regular black hole into a whole regular horizonless spacetime.

On the other hand, there is a correspondence between the properties of anti–de Sitter (AdS) spacetime and conformal field theory, the so-called AdS-CFT correspondence [32]. It provides possible insights for physicists to explore quantum gravity and grand unified theories. It also offers a potential platform for experimentalists to study quantum effects in flat spacetime using gravitational theory methods. As a result of the correspondence, the study of AdS spacetime has attracted the attention of many researchers [33].

This paper investigates the perturbative properties of regular horizonless anti–de Sitter spacetime observing a probe scalar field evolving in this geometry. Since there is no event horizon in this spacetime, the tortoise coordinate, denoted as $r_* \equiv \int_0^r \frac{dy}{f(y)}$, exists in the range of $[0, r_*^{\max}]$, where $r_*^{\max}$ is a finite positive number. Consequently, the perturbations in this spacetime exhibit significant differences with respect to those in black holes and ordinary stars in asymptotically flat spacetime.

In Sec. II, we will review how to derive the general relationship between C_M and $\mathcal{L}(F)$ by using nonlinear electromagnetic theory. We will take several common regular spacetimes as examples to show the behavior of C_M when $r \to \infty$. In Sec. III, we construct the scalar field perturbations in regular horizonless anti–de Sitter spacetime and show the corresponding boundary conditions. Numerical calculations and analysis are performed in Sec. IV. In Sec. V are included discussions and conclusions.

II. REGULAR BLACK HOLE SOLUTION AND NONLINEAR ELECTRODYNAMICS

After Bardeen proposed the idea of regular black holes, it was discovered that Bardeen black holes could be obtained by choosing, appropriately, the form of the nonlinear electromagnetic field in nonlinear Einstein-Maxwell theory. Subsequently, the metrics of different regular black holes have been derived by selecting different forms of nonlinear electromagnetic fields. In four-dimensional general relativity, the action with a nonlinear electromagnetic field is given by

$$S = \frac{1}{16\pi}\int dx^4\sqrt{-g}[R - \mathcal{L}(F)], \tag{2.1}$$

where the nonlinear electromagnetic term $\mathcal{L}(F)$ is a function of $F \equiv F_{\mu\nu}F^{\mu\nu}$. From the action, the Einstein

field equations (or gravitational field equations) and nonlinear Maxwell equations (nonlinear electromagnetic equations) are

$$R_{\mu\nu}-\frac{1}{2}g_{\mu\nu}R=2\frac{\partial\mathcal{L}}{\partial F}g^{\alpha\beta}F_{\alpha\mu}F_{\beta\nu}-\frac{1}{2}g_{\mu\nu}\mathcal{L}(F),$$
$$\nabla_{\nu}\left[\frac{\partial\mathcal{L}}{\partial F}F^{\mu\nu}\right]=0. \tag{2.2}$$

According to the static spacetime metric with magnetic charge, we substitute Eqs. (1.1)–(1.3) into the gravitational field equations and electromagnetic field equations and find that the electromagnetic field equation is satisfied automatically and the gravitational field equations yield the following relationship:

$$C_M'=\frac{dC_M(r)}{dr}=r^2\mathcal{L}(F), \tag{2.3}$$

where

$$F=2Q_m^2/r^4$$
$$\text{or}\quad r=2^{1/4}Q_m^{1/2}/F^{1/4}. \tag{2.4}$$

By comparing Eqs. (2.3) and (1.4), we find $\mathcal{L}(F)=\frac{4\pi}{M}\rho$ in a static spacetime metric with magnetic charge, where $\mathcal{L}(F)$ plays the role of the energy density ρ.

Getting the linear form $\mathcal{L}(F)=F$, we find that the factor $C_M=1-\frac{Q_m^2}{2Mr}$ and

$$f(r)=1-\frac{2M}{r}+\frac{Q_m^2}{r^2}. \tag{2.5}$$

It is no other than a metric of Reissner-Nordström-like spacetime with static magnetic charge Q_m. This spacetime is singular at $r=0$, so it implies that $\mathcal{L}(F)$ cannot be linear in a regular spacetime.

Although it is not very difficult to obtain the form of $f(r)$ for a regular spacetime metric from the assumption of $\mathcal{L}(F)$, a simpler method is to use Eq. (2.3), which allows us to conveniently determine the form of $\mathcal{L}(F)$ by choosing the form of C_M.

Let us take Hayward regular spacetime as an example. The C_M in the metric is written as

$$C_M=\frac{r^3}{r^3+2\beta^2}. \tag{2.6}$$

By substituting Eqs. (2.4) and (2.6) into Eq. (2.3), we obtain

$$\mathcal{L}(F)=\frac{6\sqrt{2}M\beta^2F^{3/2}}{(Q_m^{3/2}+2^{1/4}\beta^2F^{3/4})^2}. \tag{2.7}$$

To eliminate Q_m and M from the equation, we set

$$Q_m^{3/2}=\gamma\beta^2=2\sigma M, \tag{2.8}$$

and, therefore,

$$\mathcal{L}(F)=\frac{3\sqrt{2}\gamma F^{3/2}}{\sigma(\gamma+2^{1/4}F^{3/4})^2}, \tag{2.9}$$

where γ and σ are undetermined parameters in the action $\mathcal{L}(F)$. Thus,

$$f=1-\frac{2M_0}{r}-\frac{4\sigma^{-1}Q_m^{3/2}r^2}{r^3+2\gamma^{-1}Q_m^{3/2}}. \tag{2.10}$$

In Eq. (2.10), $M_{\rm ADM}\equiv M_0+M_{\rm EM}\equiv M_0+\frac{Q_m^{3/2}}{2}$, where $M_{\rm EM}$ is the electromagnetic mass caused by electromagnetic interactions. When $M_0=0$ in the equation above, the black hole metric reduces to the Hayward regular metric without divergent curvature at $r=0$.

Looking at it from another viewpoint, according to Eq. (2.8), we can choose

$$f=1-\frac{2Mr^2}{r^3+4\gamma^{-1}\sigma M}. \tag{2.11}$$

In this case, although M can be interpreted as the ADM mass of the black hole, Q_m and β^2 are determined after $\mathcal{L}(F)$ is given. Here, in this paper, we will adopt this viewpoint to explain the regular horizonless spacetime metric derived from the nonlinear Einstein-Maxwell theory. Therefore, it is important to note that, while Q_m and β^2 in the metric contain γ and σ, these two parameters are fixed once the action is determined. Once the action is fixed, $Q_m=Q_m(M)$ and $\beta=\beta(M)$ depend on only the spacetime mass M.

In general, when selecting a regular black hole in a regular spacetime, we aim for the black hole metric to match the Schwarzschild metric at infinity. This is because the spacetime must satisfy the requirements of the post-Newtonian approximation. However, at $r=0$, $f(r)$ remains finite. Therefore, C_M needs to satisfy the conditions

$$\frac{C_M(r)}{r}=\begin{cases}0, & r=0,\\ \frac{1}{r}, & r\to\infty.\end{cases} \tag{2.12}$$

However, the regular spacetime solution should satisfy more conditions. As we all know, regular spacetime requires that there are no singularities at center $r=0$ and at radial infinity $r\to\infty$, so the three scalar quantities about curvatures $R=g^{\mu\nu}R_{\mu\nu}$, $\mathbb{R}=R_{\alpha\beta}R^{\alpha\beta}$, and $\mathscr{R}=R_{\alpha\beta\gamma\sigma}R^{\alpha\beta\gamma\sigma}$ must remain finite.

In the case of a static spacetime with magnetic charge, when we substitute Eqs. (1.1) and (1.2) into the

aforementioned scalar quantities, and we have

$$R = \frac{2M}{r^2}\left(2C'_M + rC''_M\right),$$
$$\mathbb{R} = \frac{2M^2}{r^4}\left(4C'^2_M + r^2C''^2_M\right),$$
$$\mathscr{R} = \frac{4M^2}{r^6}\left[12C^2_M + 4rC_M\left(rC''_M - 4C'_M\right) + r^2\left(r^2C''^2_M - 4rC'_MC''_M + 8C'^2_M\right)\right]. \quad (2.13)$$

On the other hand, if we require the action to be finite, the scalar $\mathcal{L}(F)$ must also remain finite at any position. Near $r = 0$, we assume $C_M \sim r_0^\alpha + \mathcal{O}$ and substitute this expression into the scalar quantities. By expanding around $r = 0$, we find that if the scalar fields do not diverge, then α must satisfy the condition $\alpha_0 \geq 3$. At infinity, considering that in an asymptotically flat spacetime the nonlinear electromagnetic field effects are not significant, we can assume $\mathcal{L}(F)/F = F_C|_{r\to\infty}$, where F_C is a finite constant. If $F_C \neq 0$, it implies that the nonlinear electromagnetic field effect in curved spacetime and the nonlinear electromagnetic field reduces to a linear electromagnetic field in asymptotically flat spacetime. If $F_C = 0$, it signifies that the nonlinear electromagnetic field completely vanishes at infinity. Therefore, let us assume that, at infinity, $C_M - 1 \sim r^{\alpha_{\rm inf}} + \mathcal{O}$. Substituting this into the scalar quantities, we require $\alpha_{\rm inf} \leq -1$ at infinity.

In conclusion, we obtain the conditions for regular spacetime as follows:

$$\left.\frac{C_M(r)}{r^3}\right|_{r\to 0} \not\to \infty,$$
$$\left[C_M(r) - 1\right]r|_{r\to\infty} \not\to \infty. \quad (2.14)$$

By choosing a function $C_M(r)$ that satisfies Eqs. (2.12) and (2.14), we can obtain a metric of a static regular spacetime with magnetic charge. Subsequently, we can determine the specific form of the nonlinear electromagnetic field $\mathcal{L}(F)$ based on Eqs. (2.3) and (2.4). For example, we can choose

$$C_M = \mathrm{Erf}^3\left(\frac{r}{\beta^2}\right), \quad (2.15)$$

where $\mathrm{Erf}(r) \equiv \frac{2}{\sqrt{\pi}}\int_0^r e^{-y^2}dy$ is the error function, so the regular black hole is given by

$$f = 1 - \frac{2M}{r}\mathrm{Erf}^3\left(\frac{r}{\beta^2}\right). \quad (2.16)$$

By using the method, we can even transform various regular spacetime with metric forms satisfying Eq. (1.1) into regular spacetime with magnetic charge. For example, Ref. [20] proposed a regular black hole without magnetic charge. Nevertheless, we can still use the above procedure with nonlinear electrodynamics to obtain a regular black hole with magnetic charge, and the metric has the same form as compared to this black hole.

In Table I, we have listed several common black hole metrics, which can be derived by the corresponding nonlinear electromagnetic field action $\mathcal{L}(F)$ using the aforementioned procedure.

Finally, let us discuss the properties of the event horizon in a regular black hole. If the regular spacetime still represents a black hole, it is necessary for the spacetime to possess an event horizon. Let us assume the position of the event horizon is at $r = r_p > 0$. Therefore, the metric of the regular black hole can be rewritten as

TABLE I. The metrics of some famous regular black holes.

Authors	$C_M(r)$	Reference	$\mathcal{L}(F)$	M and Q_m
Bardeen	$\frac{r^3}{(r^2+\beta^2)^{3/2}}$	[14]	$\frac{6\gamma F^{5/4}}{\sigma(\sqrt{2}\gamma^{2/3}+\sqrt{F})^{5/2}}$	$Q_m^{3/2} = \gamma\beta^3 = 2\sigma M$
Ayon-Beato and Garcia	$\frac{r^3}{(r^2+\beta^2)^{3/2}} - \frac{\beta^2 r^3}{2M(r^2+\beta^2)^2}$	[16]	$2F\frac{\sqrt{2}\gamma^{\frac{2}{3}}-3\sqrt{F}+3\frac{\gamma}{\sigma}F^{\frac{1}{4}}\sqrt{\sqrt{2}\gamma^{\frac{2}{3}}+\sqrt{F}}}{(\sqrt{2}\gamma^{2/3}+\sqrt{F})^3}$	$Q_m^{3/2} = \gamma\beta^3 = 2\sigma M$
Hayward	$\frac{r^3}{r^3+2\beta^2}$	[17]	$\frac{3\sqrt{2}\gamma F^{3/2}}{\sigma(\gamma+2^{1/4}F^{3/4})^2}$	$Q_m^{3/2} = \gamma\beta^2 = 2\sigma M$
Berej *et al.*	$1 - \tanh\left(\frac{\beta^2}{2Mr}\right)$	[18]	$\frac{F}{\gamma^{4/3}}\mathrm{sech}\left(\frac{\sigma F^{1/4}}{2^{1/4}\gamma^{4/3}}\right)^2$	$Q_m^{3/2} = \gamma\beta^{3/2} = 2\sigma M$
Dymnikova	$\frac{2}{\pi}\left[\arctan\left(\frac{r}{r_0}\right) - \frac{r_0 r}{r^2+r_0^2}\right]$	[19]	$\frac{8\gamma F}{\sigma(2\gamma^{4/3}\pi+2\sqrt{2}\pi\gamma^{2/3}\sqrt{F}+\pi F)}$	$Q_m^{3/2} = \gamma r_0^3 = 2\sigma M$
Dymnikova	$1 - e^{-r^3/r_0^2 r_g}$	[20]	$\frac{6\gamma}{\sigma}e^{-\frac{2^{3/4}}{F^{3/4}}\gamma}$	$Q_m^{3/2} = \gamma r_0^2 r_g = 2\sigma M$
Lin *et al.*	$1 - e^{-r^{3(1+n)}/A}$ with $n \geq 0$	[21]	$3\frac{2^{1+\frac{3n}{4}}(n+1)\gamma^{n+1}}{F^{3n/4}}e^{-\left(\frac{2\gamma^{\frac{4}{3}}}{F}\right)^{\frac{3(n+1)}{4}}}$	$Q_m^{3/2} = \gamma A^{\frac{1}{n+1}} = 2\sigma M$
The example in this paper	$\mathrm{Erf}^3\left(\frac{r}{\beta^2}\right)$	Eq. (2.15)	$\frac{6\gamma^{\frac{1}{3}}}{\sigma}\sqrt{\frac{2F}{\pi}}e^{-\frac{\sqrt{2}\gamma^{\frac{2}{3}}}{\sqrt{F}}}\mathrm{Erf}^2\left[\left(\frac{2\gamma^{\frac{4}{3}}}{F}\right)^{\frac{1}{4}}\right]$	$Q_m^{3/2} = \gamma\beta^6 = 2\sigma M$

$$f(r) = 1 - \frac{r_p C_M(r)}{r C_M(r_p)}. \tag{2.17}$$

The above equation requires $C_M(r_p) > 0$ as a regular black hole, and the temperature of the black hole is given by

$$T_H = \frac{1 - r_p C_p}{4\pi r_p}, \tag{2.18}$$

where $C_p = C'_M/C_M|_{r=r_p}$.

The discussion above refers to the metric of asymptotically flat spacetime. If we add a cosmological constant term to the action, the action becomes

$$S = \frac{1}{16\pi}\int dx^4\sqrt{-g}\left[R + \frac{6}{l_0^2} - \mathcal{L}(F)\right], \tag{2.19}$$

where $\frac{3}{l_0^2} \equiv -\Lambda$, so we can obtain asymptotically (anti–)de Sitter solutions. For $l_0^2 > 0$, it corresponds to anti–de Sitter spacetime, while $l_0^2 < 0$ corresponds to de Sitter spacetime case. The (anti–)de Sitter solutions are obtained simply by adding a term $\frac{r^2}{l_0^2}$ to Eq. (1.2) [34–37], namely,

$$f_\Lambda(r) = 1 - \frac{2M}{r}C_M(r) + \frac{r^2}{l_0^2}. \tag{2.20}$$

However, the relation between C_M and $\mathcal{L}(F)$ remains unchanged. Additionally, curvature scalars quantities are

$$\begin{aligned} R_\Lambda &= R_0 - \frac{12}{l_0^2}, \\ \mathbb{R}_\Lambda &= \mathbb{R}_0 - \frac{12M}{l_0^2 r^2}\left(2C'_M + rC''_M\right) + \frac{36}{l_0^4}, \\ \mathscr{R}_\Lambda &= \mathscr{R}_0 - \frac{8M}{l_0^2 r^2}\left(2C'_M + rC''_M\right) + \frac{24}{l_0^4}, \end{aligned} \tag{2.21}$$

where R_0, $\mathbb{R}_0$, and $\mathscr{R}_0$ are the curvature invariants as derived from asymptotically flat spacetime (2.13). Following the same idea as before, we find that C_M still satisfies the conditions Eqs. (2.12) and (2.14).

III. SCALAR PERTURBATION IN REGULAR ANTI–DE SITTER SPACETIME

In this section, we study the dynamical behavior of scalar field perturbations in spacetimes with a negative cosmological constant obtained using the method previously discussed. They are the Hayward solution, Bardeen solution, Berej solution, and Erf solution asymptotically anti–de Sitter, respectively. The component of metrics for these four types of regular spacetimes are

$$\begin{aligned} f_{\text{Hayward}} &= 1 - \frac{2Mr^2}{r^3 + 2\beta^2} + \frac{r^2}{l_0^2}, \\ f_{\text{Bardeen}} &= 1 - \frac{2Mr^2}{(r^2+\beta^2)^{3/2}} + \frac{r^2}{l_0^2}, \\ f_{\text{Berej}} &= 1 - \frac{2M}{r}\left[1 - \tanh\left(\frac{\beta^2}{2Mr}\right)\right] + \frac{r^2}{l_0^2}, \\ f_{\text{Erf}} &= 1 - \frac{2M}{r}\text{Erf}^3\left(\frac{r}{\beta^2}\right) + \frac{r^2}{l_0^2}. \end{aligned} \tag{3.1}$$

Choosing $M = 1/2$ and $\Lambda = -3$, for example, these regular spacetimes become horizonless, i.e., without event horizon, if we require that $\beta > 0.196625$ for the Hayward case, $\beta > 0.327414$ for the Bardeen case, $\beta > 0.496927$ for the Berej case, and $\beta > 0.696562$ for the Erf case.

Without loss of generality, we set $M = 1/2$, $Q_m = 1$, $\Lambda = -3$ ($l_0 = 1$), and $\gamma = \sigma = 1$, so $\beta = 1$. Thus, the horizonless condition is satisfied by all four solutions.

We will display the plots of $f_\Lambda = f_\Lambda(r)$, $r_* = r_*(r)$, and $C_M = C_M(r)$ for this case in Fig. 1. It can be seen that, in the spacetime metrics for these cases, there is no event horizon present. Therefore, they are regular horizonless spacetimes, and the tortoise coordinate $r_* \equiv \int_0^r \frac{dy}{f_\Lambda(y)}$ has upper and lower bounds for its values.

Here, it has been considered the simplest case of scalar field perturbation. Therefore, substituting the regular horizonless spacetime metrics into the massless scalar field equation,

$$\frac{1}{\sqrt{-g}}\frac{\partial}{\partial x^\mu}\left(\sqrt{-g}g^{\mu\nu}\frac{\partial}{\partial x^\nu}\Phi\right) = 0, \tag{3.2}$$

we get the equation of motion as

$$-\frac{\partial^2\psi}{\partial t^2} + \frac{\partial^2\psi}{\partial r_*^2} - V(r(r_*))\psi = 0, \tag{3.3}$$

where

$$\begin{aligned} r_*(r) &\equiv \int_0^r \frac{dy}{f_\Lambda(y)} \in [0, r_*^{\max}], \\ V(r) &= \frac{f_\Lambda(r)}{r^2}\left[L(L+1) + r\frac{d}{dr}f_\Lambda(r)\right]. \end{aligned} \tag{3.4}$$

Figure 2 shows the effective potential $V = V(r_*)$ with $L = 0, 1, 2, 3$. It can be observed that $V \to \infty$ as $r \to \infty$ (namely, $r_* \to r_*^{\max}$). On the other hand, as $r \to 0$ (namely, $r_* \to 0$), for $L = 0$ the value of $V(r_* = 0)$ remains finite, while for $L \geq 1$ it diverges.

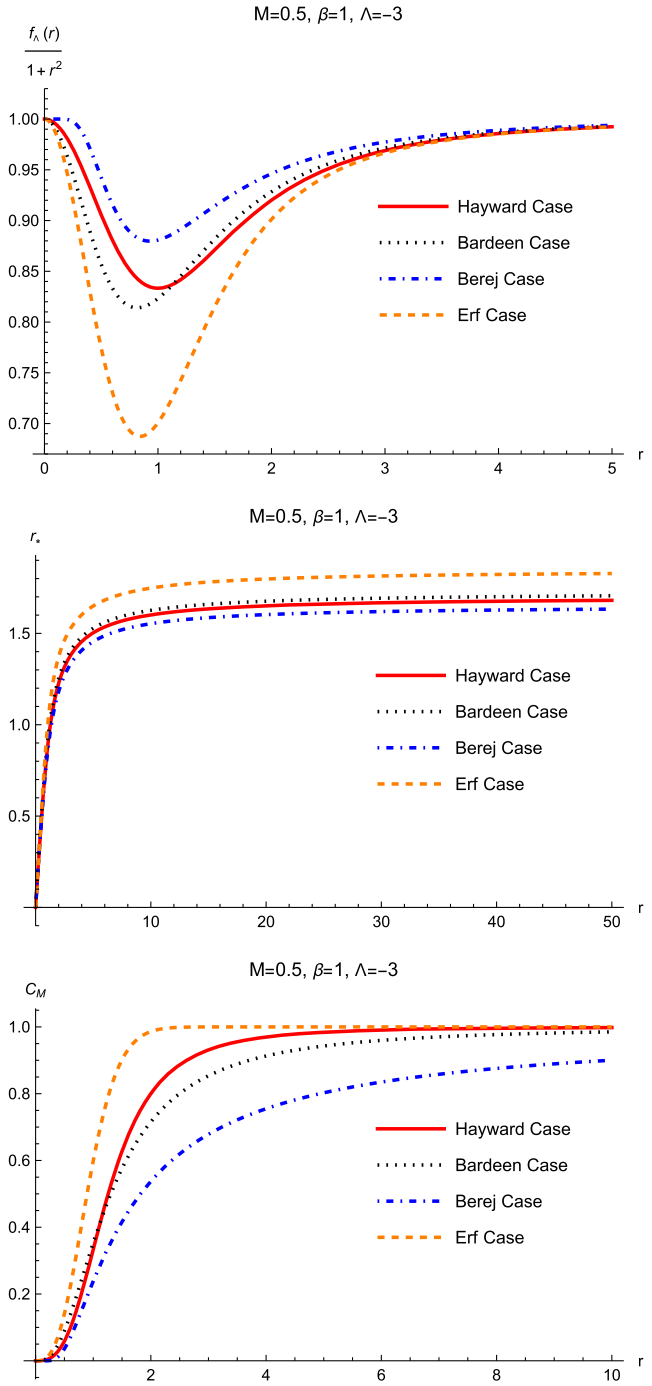

FIG. 1. $f_\Lambda = f_\Lambda(r)$, $r_* = r_*(r)$, and $C_M = C_M(r)$ at the Hayward case, Bardeen case, Berej case, and Erf case, respectively. In order to show the differences between the four types of regular horizonless spacetime, we display the functional form of $\frac{f_\Lambda(r)}{1+r^2}$ at the top of the panel. It is observed that $f_\Lambda(r) \neq 0$ within the range of values. The figure of $C_M = C_M(r)$ indicates that the values of the metrics $f = f(r)$ are limited within a finite range.

In order to study the asymptotic behavior of the regular horizonless spacetime at its center and at infinity, we can expand V at $r = 0$ and $r \to \infty$ and obtain the following expressions:

$$\psi(r \to 0) = C_A r^{L+1} + C_B r^{-L},$$
$$\psi(r \to \infty) = C_a r^{-2} + C_b r. \tag{3.5}$$

In order to ensure that the wave function is finite at these two points, we set $C_B = C_b = 0$. Therefore, the boundary conditions for Eq. (3.3) are

$$\psi(r \to 0) \to 0,$$
$$\psi(r \to \infty) \to 0. \tag{3.6}$$

Let us analyze Eq. (3.3) further. It can be observed that, if V vanishes, the equation becomes a standard wave equation with velocity of waves $f_\Lambda^{-1}(r)\frac{dr}{dt} = \frac{dr_*}{dt} = c = 1$. It is worth noting that $r_* \in [0, r_*^{\max}]$, which means that the wave can propagate to any position in r_* within a finite amount of time. Furthermore, considering that $r \to r_*^{\max}$ corresponds to infinity in anti–de Sitter spacetime, the scalar field phase velocity $v = \frac{dr}{dt} = f_\Lambda(r(r_*))\frac{dr_*}{dt}$ goes to infinity at radial infinity.

Now let us qualitative study Eq. (3.3) with the potential function V. First, by using the Fourier transform, we can set $\psi = e^{-i\omega t}\Psi(r_*)$ and expand the effective potential around a point $r_* = r_0$ as $V = V(r_0) + \mathcal{O}(V'(r_0)) \equiv V_0 + \mathcal{O}(V'(r_0))$. After neglecting higher-order terms and substituting it into Eq. (3.3), we have

$$\psi = e^{-i\omega t \pm i\sqrt{\omega^2 - V_0} r_*} = e^{-i\omega\left[t \pm \left(\frac{\omega}{\sqrt{\omega^2 - V_0}}\right)^{-1} r_*\right]}. \tag{3.7}$$

This means that, for a wave with frequency ω, the wave speed is given by $v_* = \frac{dr_*}{dt} = f_\Lambda^{-1}(r)\frac{dr}{dt} = \frac{\omega}{\sqrt{\omega^2 - V_0}}$. When $V_0 = 0$, the wave speed $v_* = c = 1$. When $V_0 > 0$, the wave speed v_* is greater than $c = 1$. When $V_0 = \omega^2$, the wave speed goes to infinite, indicating the scalar field becomes an action at a distance. When $V_0 > \omega^2$, not only does the action not require time to propagate, but its perturbation amplitude may also goes to zero or diverge. Based on the values of V shown in Fig. 2, we can conclude that any scalar perturbation at any position can propagate to any position in $r \in [0, r_*^{\max}]$ in a finite time.

Given that the range of $r_* < 0$ and $r_* > r_*^{\max}$ is physically meaningless, it can be effectively regarded as

$$\psi(r_* < 0) = \psi(r_* > r_*^{\max}) = 0. \tag{3.8}$$

This is exactly the boundary condition for an infinite potential well in quantum mechanics. Therefore, the Klein-Gordon equation of a regular horizonless anti–de Sitter spacetime can be considered as a quantum mechanical problem with an asymmetric infinite potential well, whose boundary condition is given by Eq. (3.8), and its corresponding effective potential function can be equivalently written as

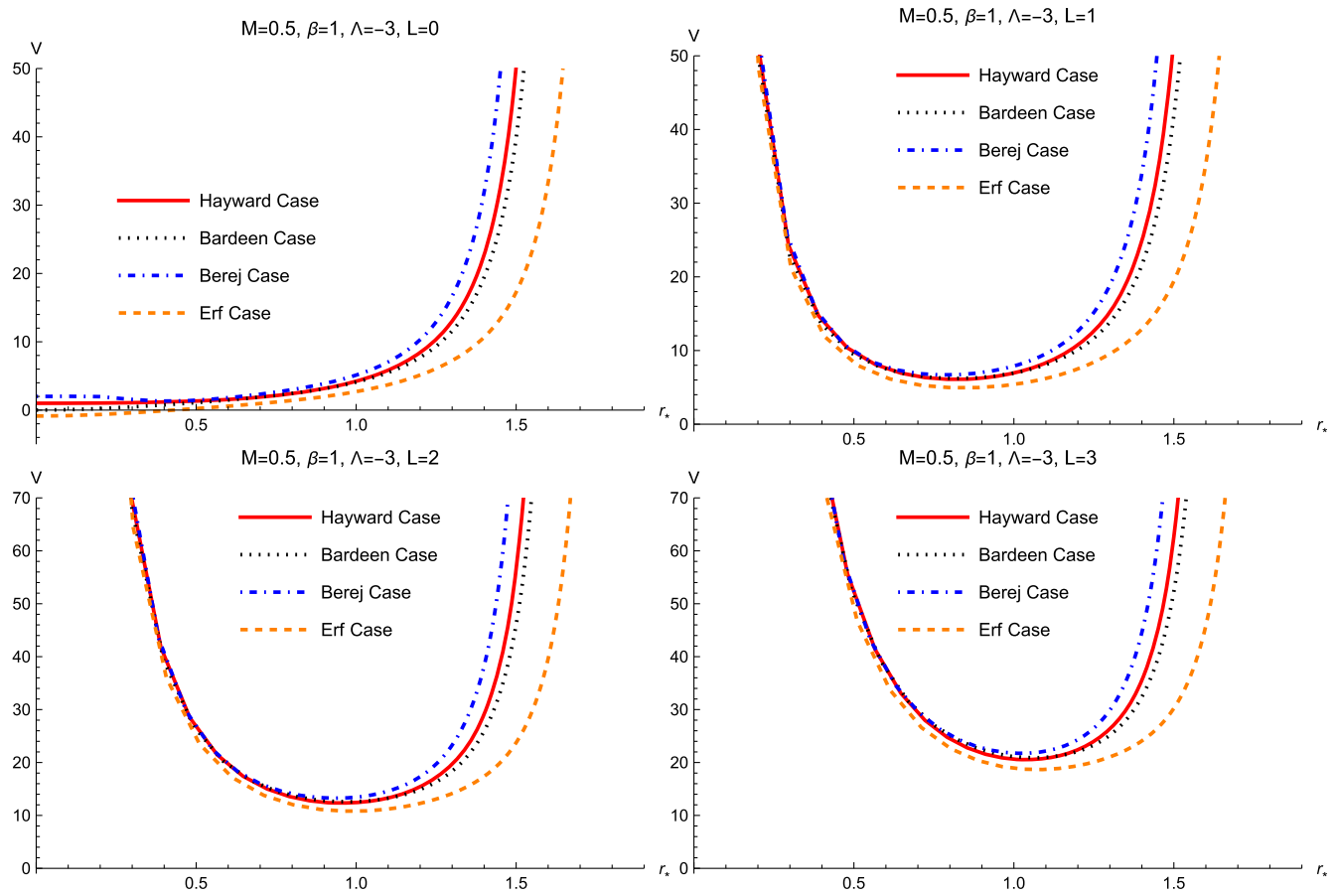

FIG. 2. The effective potential $V = V(r_*)$ for the scalar field with $L = 0$, 1, 2, 3.

$$V(r) = \begin{cases} \infty & r_* < 0, \\ \frac{f_\Delta}{r^2}\left[L(L+1) + r f'_\Lambda\right] & 0 \geq r_* \geq r_*^{\max}, \\ \infty & r_* > r_*^{\max}. \end{cases} \tag{3.9}$$

Under the assumptions made above, Eq. (3.3) can be put in the format of an eigenvalues equation, resulting in

$$\frac{d^2\Psi}{dr_*^2}(r_*) + \left[\omega^2 - V(r(r_*))\right]\Psi(r_*) = 0, \tag{3.10}$$

whose eigenfunctions are denoted by Ψ and eigenvalues by ω^2. Let us first analyze the orthogonality and completeness of the above equation using the Sturm-Liouville theory.

The orthogonality of Eq. (3.10) with the boundary condition (3.8) can be proved by taking two different solutions of Eq. (3.10), which are given by

$$\begin{aligned} \mathbb{L}_n[\Psi, r_*] &\equiv \frac{d^2}{dr_*^2}\Psi_n - V(r_*)\Psi_n = -\omega_n^2\Psi_n, \\ \mathbb{L}_m[\Psi, r_*] &\equiv \frac{d^2}{dr_*^2}\Psi_m - V(r_*)\Psi_m = -\omega_m^2\Psi_m \end{aligned} \tag{3.11}$$

and whose eigenvalues are $\omega_n \neq \omega_m$ and eigenfunctions are $\Psi_n \neq \Psi_m$. Therefore,

$$\begin{aligned} \mathbb{Q} &\equiv \int_0^{r_*^{\max}} \{\Psi_m \mathbb{L}_n[\Psi, r_*] - \Psi_n \mathbb{L}_m[\Psi, r_*]\} dr_* \\ &= -(\omega_n^2 - \omega_m^2)\int_0^{r_*^{\max}} \Psi_m \Psi_n dr_*. \end{aligned} \tag{3.12}$$

We can obtain, by integrating by parts,

$$\begin{aligned} \mathbb{Q} = &\left[\Psi_m \frac{d\Psi_n}{dr_*} - \Psi_n \frac{d\Psi_m}{dr_*}\right]_0^{r_*^{\max}} \\ &- \int_0^{r_*^{\max}} \left[\frac{d\Psi_n}{dr_*} d\Psi_m - \frac{d\Psi_m}{dr_*} d\Psi_n\right] = 0 \end{aligned} \tag{3.13}$$

because of the boundary conditions (3.8) $\Psi(r_* = 0) = \Psi(r_* = r_*^{\max}) = 0$ and $d\Psi_n = \frac{d\Psi_n}{dr_*} dr_*$. From the above relation, we have

$$\int_0^{r_*^{\max}} \Psi_m \Psi_n dr_* = -\frac{\mathbb{Q}}{\omega_n^2 - \omega_m^2} = 0 \quad \text{for } n \neq m. \tag{3.14}$$

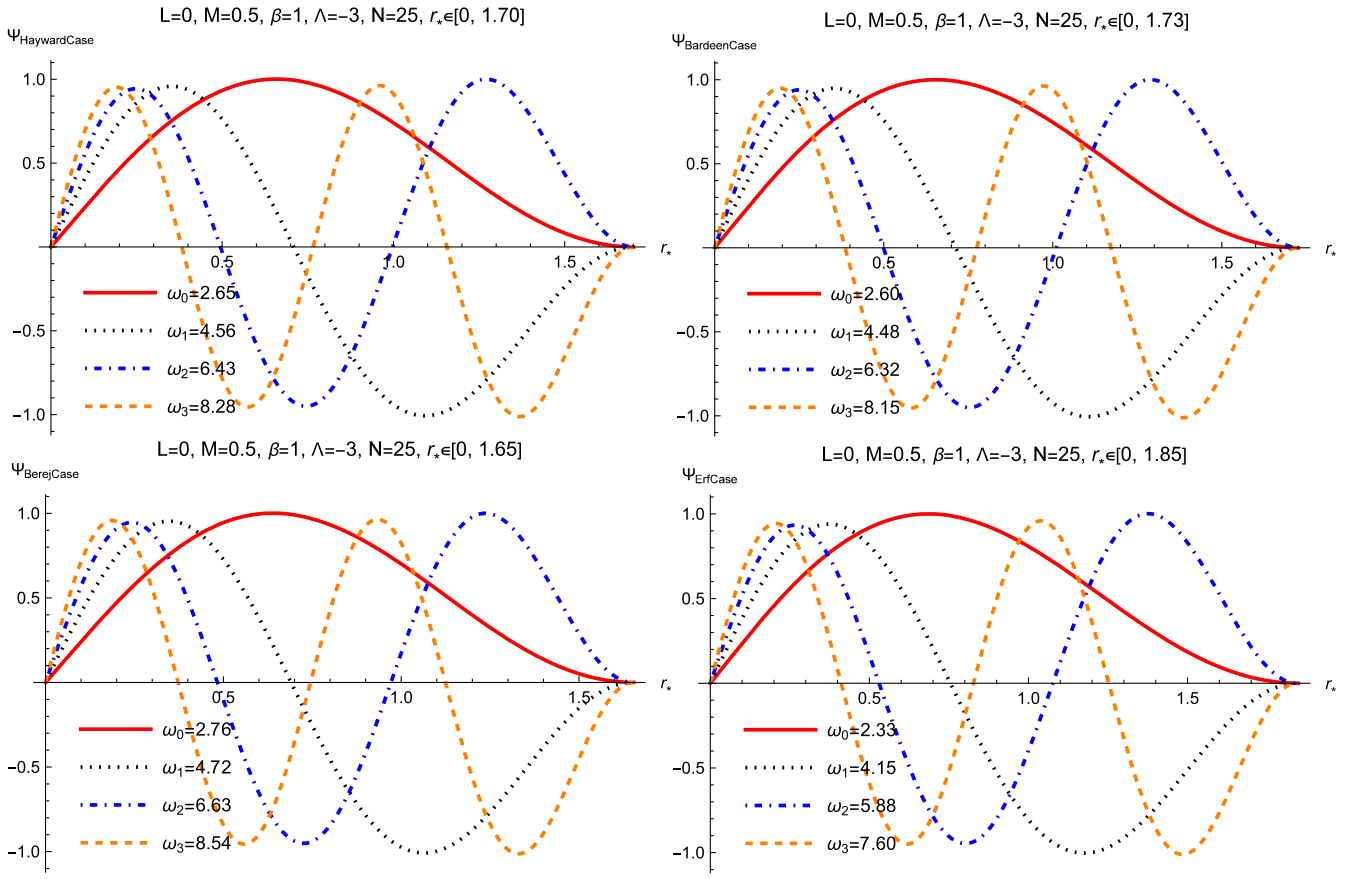

FIG. 3. Matrix method for scalar normal modes of Hayward, Bardeen, Berej, and Erf regular horizonless AdS spacetimes with $L = 0$.

On the other hand, we can set

$$I_n \equiv \int_0^{r_*^{\max}} \Psi_n^2 dr_* \tag{3.15}$$

so that

$$\int_0^{r_*^{\max}} \Psi_m \Psi_n dr_* = \delta_{nm} I_n. \tag{3.16}$$

It means that the eigenfunctions set $\{\Psi_i\}$ satisfying an orthogonality condition.

Next, let us prove that the eigenfunction set $\{\Psi_i\}$ is complete, which means that any function $\Phi(r_*)$ can be expanded as

$$\Phi(r_*) = \sum_n C_n \Psi_n(r_*) \tag{3.17}$$

with constant coefficients C_n. In order to find C_n, we can calculate the integral as follows:

$$\begin{aligned}\int_0^{r_*^{\max}} \Psi_m \Phi dr_* &= \sum_n C_n \int_0^{r_*^{\max}} \Psi_m \Psi_n dr_* \\ &= \sum_n C_n \delta_{nm} I_n = I_m C_m\end{aligned} \tag{3.18}$$

or

$$C_n = \frac{1}{I_n} \int_0^{r_*^{\max}} \Psi_n \Phi dr_*. \tag{3.19}$$

Therefore, the eigenfunction set $\{\Psi_i\}$ is complete in the range $0 \geq r \geq r_*^{\max}$. Finally, Eq. (3.10) can be written as

$$\mathcal{L}\Psi + \omega^2 \Psi = 0, \tag{3.20}$$

where $\mathcal{L}$ is a linear operator given by

$$\mathcal{L} = \frac{d}{dr_*}\left(\frac{d}{dr_*}\right) - V(r_*) \tag{3.21}$$

and ω^2 are the eigenvalues. In this format, we can treat the eigenvalue problem in the Hilbert space $L^2([0, r_*^{\max}], dr_*)$ with the scalar product given by

$$\langle h_1, h_2 \rangle = \int_0^{r_*^{\max}} \bar{h_1} h_2 dr_*. \tag{3.22}$$

In the next section, we will perform numerical calculations for above wave equation with potential $V = V(r(r_*))$.

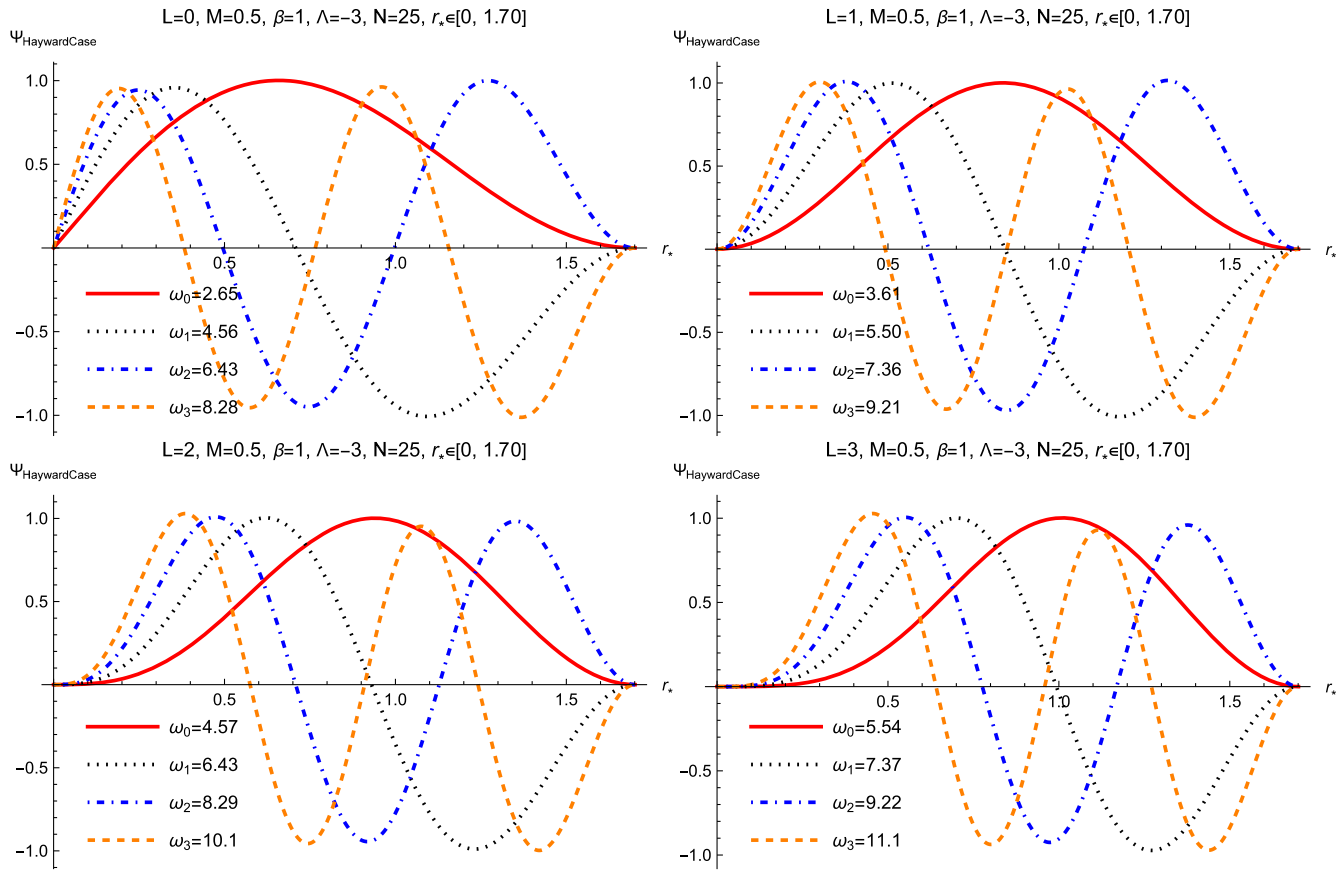

FIG. 4. Matrix method for scalar normal modes of Hayward regular horizonless AdS spacetime with $L = 0$, 1, 2, 3, respectively.

IV. NUMERICAL RESULTS

We can use either the matrix method [38–46] or the finite difference method [47–52] to calculate Eq. (3.3).

The matrix method requires one to rewrite the wave function as $\psi = e^{-i\omega t}\Psi(r_*)$ and introduces a variable transformation $x = r_*/r_*^{\max} \in [0, 1]$, so that we have

$$\Psi''(x) + [(r_*^{\max}\omega)^2 - (r_*^{\max})^2 V(r(x))]\Psi(x) = 0. \quad (4.1)$$

According to the matrix method, we can uniformly choose $N+1$ points in a grid, $x_i \in X = x_0 \equiv 0, x_1, x_2, \ldots, x_N \equiv 1$ within the interval $x \in [0, 1]$. Let us define $F = \{F_0, F_1, \ldots, F_N\}$ and $F'' = \{F_0'', F_1'', \ldots, F_N''\}$ [where $F_i = \Psi(x_i)$ and $F_i'' = \Psi''(x_i)$]. We can find the relationship between F and F'' through a high-precision difference method [38], $F'' = M_2 F$, where M_2 is an $(N+1)\times(N+1)$ square matrix, and let $\bar{M}_0$ be the $(N+1)$-dimensional identity matrix. Thus, the above equation can be written as a matrix equation:

$$\left\{M_2 + \left[(r_*^{\max}\omega)^2 - (r_*^{\max})^2 V(r(X))\right]\bar{M}_0\right\}F \equiv M(\omega)F = 0. \quad (4.2)$$

Therefore, we can determine the eigenfrequency ω by solving the determinant equation $\det(M(\omega)) = 0$. Then, we can solve for the column matrix $F = \{\Psi(x_i)\}$ and finally obtain the solution of the function $\Psi = \Psi(x) = \Psi(r_*/r_*^{\max})$ by interpolation.

Figures 3 and 4 show the time evolution of the scalar field by the matrix method. It is obvious that, in contrast to the case of asymptotically flat spacetimes or black hole spacetimes, the eigenfrequencies of the wave equation are real in the regular horizonless anti–de Sitter spacetime. This means that these oscillations do not decay over time, making them normal modes instead of quasinormal modes. The physical reason for this is that, when viewed in terms of the r_* coordinate, the region where these oscillations occur is finite. Moreover, the effective potential function Eq. (3.9) implies that all energy is completely confined within the range $0 \geq r_* \geq r_*^{\max}$. Consequently, the energy of the oscillations does not decrease, what is consistent with the results of an infinite potential well in quantum mechanics. Next, we can use these eigenfunctions as initial values to study the dynamics of scalar perturbations as they evolve over time.

In order to check the results, we use Pöschl-Teller potential $V_{\rm PT} = V_{\rm PT}(r_*)$ to fit $V(r(r_*))$, where

TABLE II. Hayward regular spacetime's normal modes frequency ω by Pöschl-Teller approximation and matrix method, respectively, where $M = 0.5$, $\beta = 1$, $\Lambda = -3$, and $r_* \in [0, 1.70086]$.

n	Matrix method	Pöschl-Teller approximation
$L = 0$	$N = 25$	$K = 0.994637$, $\lambda = 2.00013$
0	2.64698	2.76576
1	4.56353	4.61282
2	6.42852	6.45988
3	8.28425	8.30694
$L = 1$	$N = 25$	$K = 1.99766$, $\lambda = 2.00082$
0	3.61016	3.69272
1	5.49785	5.53978
2	7.35689	7.38684
3	9.21051	9.2339
$L = 2$	$N = 25$	$K = 2.99793$, $\lambda = 2.00219$
0	4.57049	4.61776
1	6.43288	6.46482
2	8.28593	8.31188
3	10.1373	10.1589
$L = 3$	$N = 25$	$K = 3.99781$, $\lambda = 2.00424$
0	5.53713	5.54307
1	7.37234	7.39013
2	9.21749	9.23719
3	11.0656	11.0843

$$V_{\mathrm{PT}}(r_*) = \alpha^2\left[\frac{K(K-1)}{\sin^2(\alpha r_*)} + \frac{\lambda(\lambda-1)}{\cos^2(\alpha r_*)}\right],$$
$$r_*^{\max} = \frac{\pi}{2\alpha}. \tag{4.3}$$

The eigenfunction and eigenvalue of above equation are given, respectively, by

$$\Psi_n(r_*) = \sin^K(\alpha r_*)\cos^\lambda(\alpha r_*) \times F\left(-n, K+\lambda+n, K+\frac{1}{2}; \sin^2(\alpha r_*)\right),$$
$$\omega_n = \alpha(K+\lambda+2n), \tag{4.4}$$

where $F(\alpha, \beta, \gamma; z)$ is a hypergeometric function. After determining the parameters K and λ, we can obtain approximate values of the normal modes frequency showed in Table II and Fig. 5.

In order to study the dynamics of scalar perturbations over time, we need to apply finite difference methods to solve Eq. (3.9). For this purpose, we set $t_i = t_0 + i\Delta t$, $r_{*j} = j\Delta r_*$, $\psi_j^i = \psi(t = t_i, r_* = r_{*j})$, and $V_j = V(r_* = r_{*j})$. Then, the master equation (3.9) becomes

$$\psi_j^{i+1} = -\psi_j^{i-1} + \frac{\Delta t^2}{\Delta r_*^2}\left(\psi_{j-1}^i + \psi_{j+1}^i\right) + \left(2 - 2\frac{\Delta t^2}{\Delta r_*^2} - \Delta t^2 V_j\right)\psi_j^i. \tag{4.5}$$

Considering that $r_* \in [0, r_*^{\max}]$, we discretize this range with $n+1$ grid points, so $\Delta r_* = r_*^{\max}/(n+1)$. Now, the boundary conditions become

$$\psi_0^i = \psi_n^i = 0. \tag{4.6}$$

After discretizing the initial conditions, we have

$$\psi_j^0 = \phi_0(x_j),$$
$$\psi_j^1 = \psi_j^0 + \Delta t\dot{\phi}_0(x_j). \tag{4.7}$$

Therefore, the calculation using the finite difference method can be performed by specifying the initial conditions $\phi_0(x_j)$ and $\dot{\phi}_0(x_j)$.

We first take the eigenfunctions calculated using the matrix method as the initial function $\psi_j^0 = \phi_0(x_j)$ and set $\dot{\phi}_0(x_j) = 0$, so $\psi_j^0 = \psi_j^1 = \phi_0(x_j)$. We then plot the results in Fig. 6, which shows that it corresponds to a standing wave. Since the energy carried by the wave cannot propagate into the regions of $r_* < 0$ and $r_* > r_*^{\max}$, the amplitude does not decrease. Additionally, the initial waveform represents an eigenfunction, which corresponds to a normal mode of the system. Hence, it matches the system's inherent vibration modes, resulting in the occurrence of standing waves.

If we change the initial condition to a Gaussian wave packet $\phi_0(x_j) = e^{-1250(r_*-0.5)^2}$ and set $\dot{\phi}_0(x_j) = 0$, we can obtain Fig. 7. In this case, since the energy is always within the range $[0, r_*^{\max}]$, the wave packet bounces back and forth within this range. This process illustrates two properties of the regular horizonless AdS spacetimes: (i) When r is very large (i.e., when r_* approaches $r_*^{\max}$), the velocity $v = dr/dt$ goes to infinity and bounces back as $r \to \infty$ (i.e., at $r_* = r_*^{\max}$). (ii) The Gaussian wave packet can clearly be decomposed into a linear combination of many eigenfunctions, implying that the eigenvalues Ψ_n $(n = 0, 1, 2, 3, \ldots)$ of the system form a complete set.

In Fig. 7, we notice a very interesting phenomenon: For the case of $L = 0$, there is a half-wave loss in the reflection of the Gaussian beam at $r_* = 0$, while in all other cases, there is no such half-wave loss in the reflections. To explain this phenomenon, let us consider the form of the potential function in Fig. 2 and Eq. (3.9). We know that the reflection interface of the Gaussian wave packet in this system is located at $r_* = 0$ and $r_* = r_*^{\max}$. When $L = 0$, in the region $0 \geq r_* \geq r_*^{\max}$, $V(r_* \to 0) = 0$, while $V(r_* < 0) \to \infty$. This is clearly a boundary between a low-density medium and a high-density medium, and the Gaussian wave packet

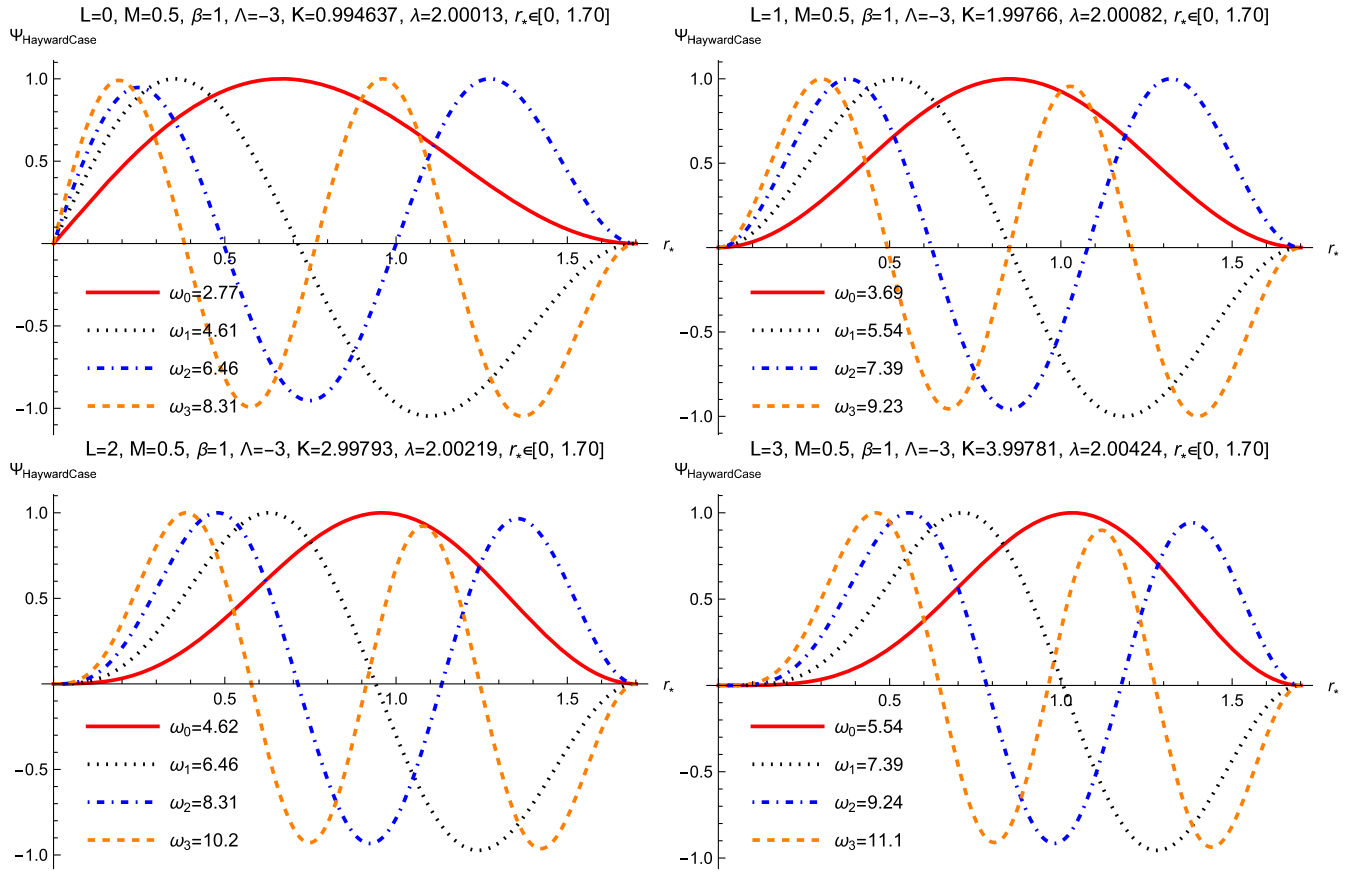

FIG. 5. Pöschl-Teller approximation for scalar normal modes of Hayward regular horizonless AdS spacetime with $L = 0$, 1, 2, 3, respectively.

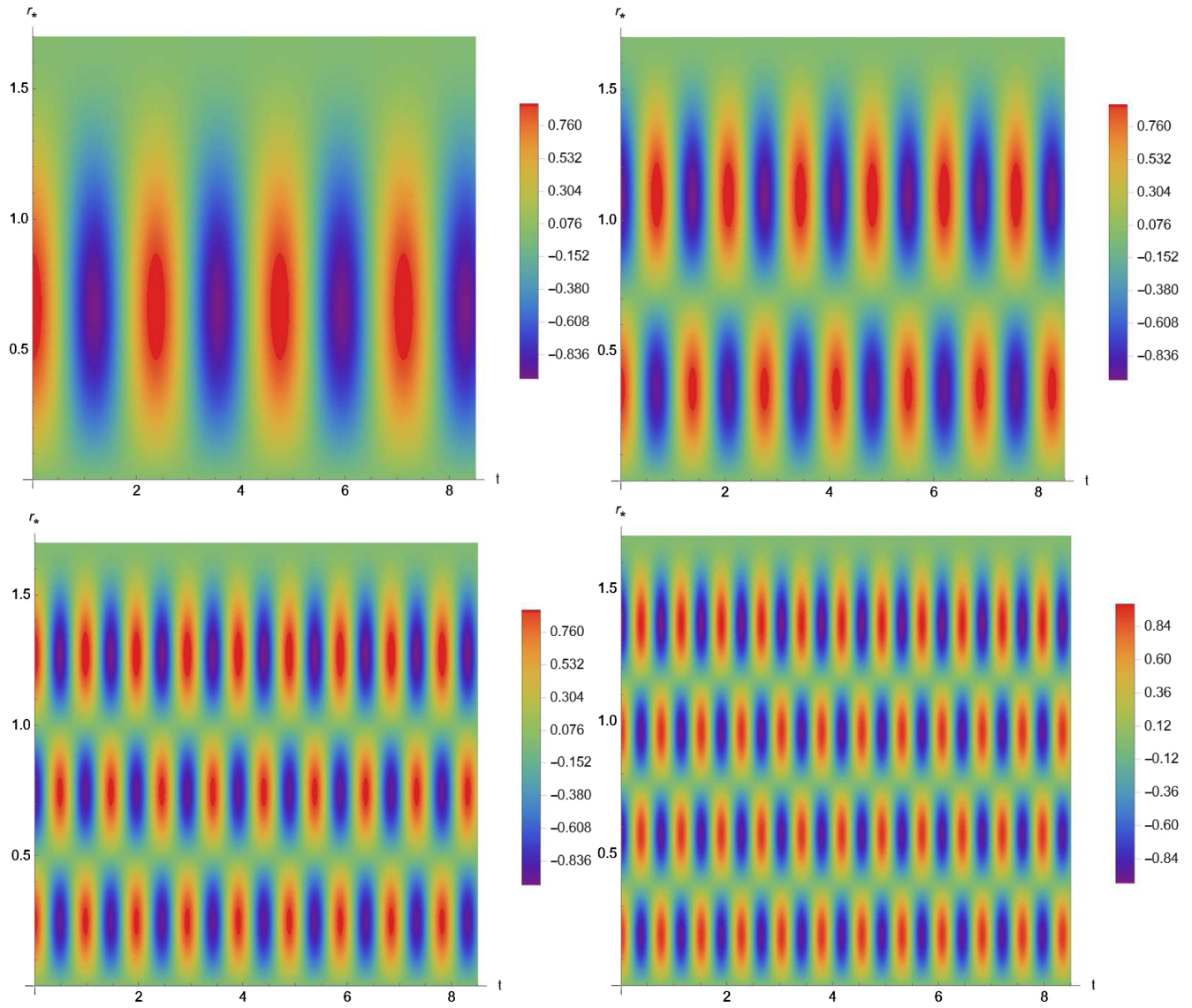

FIG. 6. Scalar standing waves of Hayward regular horizonless AdS spacetime with $L = 0$, $n = 0$ (upper left), $L = 0$, $n = 1$ (upper right), $L = 0$, $n = 2$ (bottom left), and $L = 0$, $n = 3$ (bottom right), respectively.

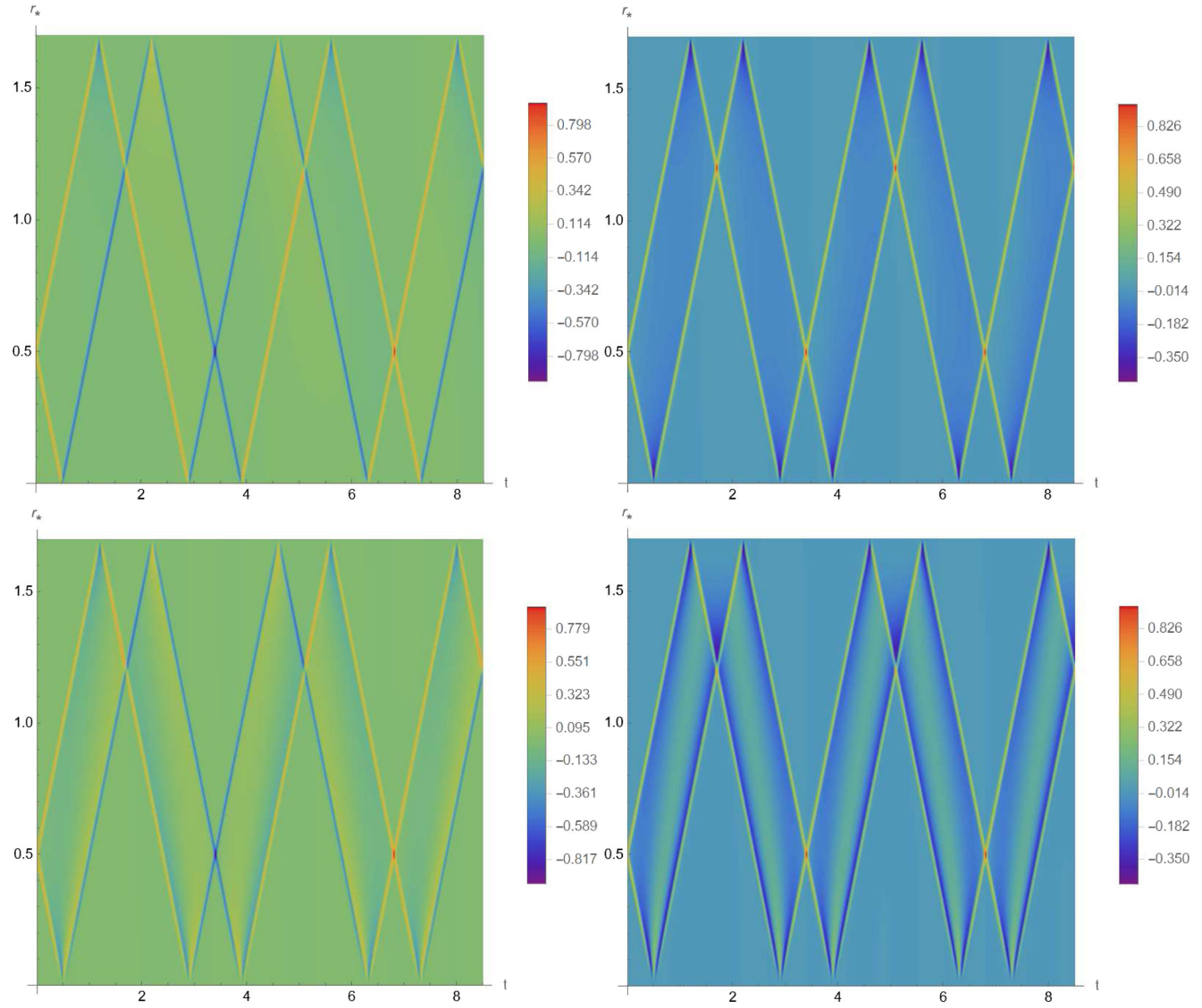

FIG. 7. The reflection process of scalar wave in Hayward regular anti-de Sitter spacetime, where $L = 0$ (upper left), $L = 1$ (upper right), $L = 2$ (bottom left), and $L = 3$ (bottom right). We can clearly see that, in the case of $L = 0$, there is a significant half-wave loss in the reflected wave at the center.

reflects on the side of the low-density medium, resulting in the occurrence of half-wave loss. On the other hand, for the case of $L \geq 1$ or at the interface $r_* = r_*^{\max}$, although $V(r_* < 0) \to \infty$ and $V(r_* > r_*^{\max}) \to \infty$, in the region $0 \geq r_* \geq r_*^{\max}$, $V(r_* = 0) \to \infty$ and $V(r_* \to r_*^{\max}) \to \infty$. Therefore, when the wave reaches the boundary, it is no longer a case of a low-density medium entering a high-density medium, and, thus, the phenomenon of half-wave loss cannot be observed.

V. CONCLUSION

In this work, we have studied scalar perturbations in the regular horizonless AdS spacetimes. We find that the range of the tortoise coordinate $r_* = \int_0^r \frac{dy}{f_\Lambda(y)}$ is limited in this spacetime, and the wave of the scalar field perturbation can propagate to any radial position in a finite amount of time, suggesting that these spacetimes allow the action at a distance in some region. Considering the physical interpretation of the tortoise coordinate, we can equivalently treat the scalar field perturbation problem in the $t - r_*$ coordinates as an infinite asymmetric potential well problem in quantum mechanics, giving rise to eigenfrequencies of normal mode solutions. Because of energy conservation, these eigenfrequencies have not an imaginary part. Initial perturbations oscillating at these eigenfrequencies lead to the appearance of standing wave phenomena. Additionally, we also observe a phenomenon of half-wave loss in reflection at $r = r_* = 0$ as $L = 0$ case. This is due to the low potential being equivalent to a low-density medium

and the high potential being equivalent to a high-density medium in electrodynamics. When the wave propagates from the low-density medium side and reflects at the interface, a half-wave loss occurs.

These unique oscillations and wave propagation phenomena in the regular horizonless AdS spacetime are clearly a result of the limited range of the tortoise coordinate r_*. If we consider an asymptotically flat spacetime where $r_*(r \to \infty) \to \infty$, then waves with a finite speed of dr_*/dt cannot propagate to infinity in a finite amount of time. Therefore, the waves cannot be reflected at infinity within a finite time, and energy in a certain region will be consumed in a finite time, preventing the formation of standing waves. As a result, there are no normal modes, but, instead, we have quasinormal modes with complex eigenfrequencies.

ACKNOWLEDGMENTS

This project was supported by National Natural Science Foundation of China (NNSFC) under Contract No. 42230207 and the Fundamental Research Funds for the Central Universities, China University of Geosciences (Wuhan) with No. G1323523064.

[1] B. P. Abbott *et al.* (LIGO Scientific and Virgo Collaborations), Phys. Rev. Lett. **116**, 061102 (2016).
[2] B. P. Abbott *et al.* (LIGO Scientific and Virgo Collaborations), Phys. Rev. Lett. **116**, 241103 (2016).
[3] B. P. Abbott *et al.* (LIGO Scientific and Virgo Collaborations), Phys. Rev. Lett. **118**, 221101 (2017).
[4] B. P. Abbott *et al.* (LIGO Scientific and Virgo Collaborations), Astrophys. J. **851**, L35 (2017).
[5] B. P. Abbott *et al.* (LIGO Scientific and Virgo Collaborations), Phys. Rev. Lett. **119**, 141101 (2017).
[6] B. P. Abbott *et al.* (LIGO Scientific and Virgo Collaborations), Phys. Rev. Lett. **119**, 161101 (2017).
[7] B. P. Abbott *et al.* (LIGO Scientific and Virgo Collaborations), Phys. Rev. X **6**, 041015 (2016).
[8] F. Acernese *et al.*, Classical Quantum Gravity **32**, 024001 (2015).
[9] B. P. Abbott *et al.* (Virgo, Fermi-GBM, INTEGRAL, and LIGO Scientific Collaborations), Astrophys. J. Lett. **848**, L13 (2017).
[10] D. R. Lorimer, M. Bailes, M. A. McLaughlin, D. J. Narkevic, and F. Crawford, Science **318**, 777 (2007).
[11] Marcelo V. dos Santos, Ricardo G. Landim, Gabriel A. Hoerning, Filipe B. Abdalla, Amilcar Queiroz *et al.*, Astron. Astrophys. **681**, A120 (2024).
[12] Zhiying Zhu, Shao-Jun Zhang, C. E. Pellicer, Bin Wang, and Elcio Abdalla, Phys. Rev. D **90**, 044042 (2014); **90**, 049904(A) (2014).
[13] A. Ashtekar and V. Petkov, *Handbook of Spacetime* (Springer, New York, 2014).
[14] J. M. Bardeen, in *Proceedings of GR5* (Tbilisi, USSR, 1968), p. 174.
[15] Z.-Y. Fan and X. Wang, Phys. Rev. D **94**, 124027 (2016).
[16] E. Ayon-Beato and A. Garcia, Phys. Lett. B **493**, 149 (2000); Phys. Rev. Lett. **80**, 5056 (1998).
[17] S. A. Hayward, Phys. Rev. Lett. **96**, 031103 (2006).
[18] W. Berej, J. Matyjasek, D. Tryniecki, and M. Woronowicz, Gen. Relativ. Gravit. **38**, 885 (2006).
[19] I. Dymnikova, Classical Quantum Gravity **21**, 4417 (2004).
[20] I. Dymnikova, Gen. Relativ. Gravit. **24**, 235 (1992).
[21] K. Lin, J. Li, S. Z. Yang, and X. T. Zhu, Int. J. Theor. Phys. **52**, 1013 (2013).
[22] C. Bambi, *Regular Black Holes, Towards a New Paradigm of Gravitational Collapse* (Springer, New York, 2023).
[23] A. Flachi and J. P. S. Lemos, Phys. Rev. D **87**, 024034 (2013).
[24] J. Li, H. Ma, and K. Lin, Phys. Rev. D **88**, 064001 (2013).
[25] K. Lin, J. Li, and S. Z. Yang, Int. J. Theor. Phys. **52**, 3771 (2013).
[26] J. Li, K. Lin, and N. Yang, Eur. Phys. J. C **75**, 131 (2015).
[27] J. Li, K. Lin, H. Wen, and W.-L. Qian, Adv. High Energy Phys. **2017**, 5234214 (2017).
[28] Hans-Peter Nollert, Classical Quantum Gravity **16**, R159 (1999).
[29] K. D. Kokkotas and B. G. Schmidt, Living Rev. Relativity **2**, 2 (1999).
[30] Emanuele Berti, Vitor Cardoso, and Andrei O Starinets, Classical Quantum Gravity **26**, 163001 (2009).
[31] R. A. Konoplya and Alexander Zhidenko, Rev. Mod. Phys. **83**, 793 (2011).
[32] Edward Witten, Adv. Theor. Math. Phys. **2**, 253 (1998).
[33] Ofer Aharony, Steven S. Gubser, Juan Martin Maldacena, Hirosi Ooguri, and Yaron Oz, Phys. Rep. **323**, 183 (2000).
[34] C. Li, C. Fang, and M. He, J. Ding, and J. Deng, Mod. Phys. Lett. A **34**, 1950336 (2019).
[35] A. G. Tzikas, Phys. Lett. B **788**, 219 (2019).
[36] S. Guo and E.-W. Liang, Classical Quantum Gravity **38**, 125001 (2021).
[37] H. El Moumni and K. Masmar, Nucl. Phys. **B973**, 115590 (2021).
[38] K. Lin and W.-L. Qian, arXiv:1609.05948.
[39] K. Lin and W.-L. Qian, Classical Quantum Gravity **34**, 095004 (2017).
[40] K. Lin and W.-L. Qian, Mod. Phys. Lett. A **32**, 1750134 (2017).
[41] K. Lin and W.-L. Qian, Chin. Phys. C **43**, 035105 (2019).
[42] K. Lin, Y. Liu, W. L. Qian, B. Wang, and E. Abdalla, Phys. Rev. D **100**, 065018 (2019).
[43] K. Lin, Y.-Y. Sun, and H. Zhang, Phys. Rev. D **103**, 084015 (2021).

[44] K. Lin and W.-L. Qian, Classical Quantum Gravity **40**, 085019 (2023).
[45] K. Lin, Phys. Rev. D **107**, 124002 (2023).
[46] K. Lin, arXiv:2306.07782.
[47] C. Gundlach, R. H. Price, and J. Pullin, Phys. Rev. D **49**, 883 (1994).
[48] C. Gundlach, R. H. Price, and J. Pullin, Phys. Rev. D **49**, 890 (1994).
[49] B. Cuadros-Melgar, J. de Oliveira, and C. E. Pellicer, Phys. Rev. D **85**, 024014 (2012).
[50] E. Abdalla, Owen Pavel Fernandez Piedra, F. S. Nunez, and J. de Oliveira, Phys. Rev. D **88**, 064035 (2013).
[51] B. Cuadros-Melgar, J. de Oliveira, and C. E. Pellicer, J. Phys. Conf. Ser. **453**, 012025 (2013).
[52] K. Linand W.-L. Qian, Chin. Phys. C **47**, 085101 (2023).